16th World Conference on Earthquake Engineering, 16WCEE 2017

Santiago Chile, January 9th to 13th 2017

Paper N° 78

Registration Code: S-Y1458899343

STATISTICAL LINEARIZATION OF FRAMES WITH THE BOUC-WEN MODEL AND AXIAL FORCE-BENDING MOMENT INTERACTION

F. Colangelo(1)

(1) *Associate Professor, DICEAA Dept., University of L'Aquila, Via Giovanni Gronchi 18, 67100 L'Aquila (AQ), Italy, felice.colangelo@univaq.it*

Abstract

Considering the probabilistic methods for seismic inelastic structural analysis, Monte Carlo simulation is a reference point where generality and accuracy are of concern. Nevertheless, simulation requires a great amount of computation that makes any extensive analysis of multi-degree-of-freedom systems almost unfeasible. Then the statistical equivalent linearization may be a sound alternative to Monte Carlo simulation. Assuming the Bouc-Wen hysteresis model in particular, may yield the equivalent linear system in analytic, closed form, which is fundamental to any efficient computation. Furthermore, such model is quite versatile because a number of extensions in the literature cover the cyclic deterioration, pinching, biaxial bending, isotropic hardening, and asymmetric strength. A novel extension is proposed in order to introduce a dependency between the resisting axial force and bending moment of a beam element to be used in seismic statistical linearization analysis of framed structures.

The lumped plasticity idealization consisting in linearly elastic beam elements and hysteretic rotational springs at their ends is considered; the Bouc-Wen model is assumed as the moment-rotation law of each spring. A second-degree parabola depending on the axial force between pure tensile and compressive strength, approximates the actual interaction diagram with the bending moment. The axial force is expressed depending on the axial stiffness and deformation of the linearly elastic beam element between the springs, which involves the translational degrees of freedom of the frame joints at the beam extremities. The resisting bending moment, i.e. the yield moment of the springs, is controlled by the parameters of the Bouc-Wen model with asymmetric strength as well as by the proposed parabola. The formulation for expected values and covariance matrix of the response quantities of the statistically equivalent linear frame is developed following the usual technique for the non-zero mean stationary problem with Gaussian processes. Non-zero mean values may come from deterministic load, asymmetric strength or both; dispersion is due to randomness of the ground motion idealized as doubly filtered white noise.

A preliminary, partial validation of the proposed model is presented, limited to the zero-mean case where the deterministic load is absent and the flexural strength is symmetric. Two portal frames are analyzed with increasing seismic intensity in the horizontal direction. These frames differ in their aspect ratio that causes different variation of the axial force in the columns under a same seismic action. Consequently, the importance of interaction between axial force and bending moment is different as well. A number of response quantities are compared: the joint translations, hysteretic rotations, dissipated energies, and several coefficients of correlation. In the frame where the effect of interaction is expected to be more important, this appears to be stressed in fact. All results from the proposed formulation are reasonable. Furthermore, Monte Carlo simulation is carried out with an elasto-plastic model provided with interaction. In this case the interaction curve is piecewise linear, as implemented in the well-known computer program DRAIN. The results from statistical linearization are consistent with the results from Monte Carlo simulation. All of these encourage further validation of the proposed model aiming at future application to actual structures.

Keywords: Bouc-Wen model; PM interaction; Statistical linearization; Stochastic structural analysis

1. Introduction

The inelastic seismic analysis of civil structures should consider randomness of the ground motion as well as uncertainty of the cyclic structural behavior. A fully probabilistic approach is still difficult and computationally demanding for current practice, but it is necessary to research. Development in the field of stochastic structural dynamics is continuing. Concerning randomness of the excitation, the existing methods may be classified as oriented to numerical characteristics or to the probability density function (PDF); about structural uncertainty, one can distinguish the perturbation approach, the orthogonal expansion, and Monte Carlo (MC) simulation [1]. The statistical equivalent linearization (SEL) [2][3] is a method of the former kind, prominent for its effective application to even large systems with actual complexity [3][4]. This method yields the response probabilistic parameters with approximation that depends on the degree of nonlinearity; nevertheless computation is orders of magnitude slighter than that necessary for MC simulation. Even if one introduces the randomness of structural properties, extensive parametric analyses, for instance those to support the code provisions, are feasible [5].

Bouc [6] and Wen [7] formulated a widely known smooth differential model suitable for representing various hysteretic cycles. Despite its great versatility, this constitutive model may yield closed-form expressions of the statistically equivalent linear system. Obviously, knowing explicitly the relationships between the system parameters and the response probabilistic parameters is a key point for any efficient implementation. This is why there are a number of extensions of the Bouc-Wen model with frequent application to SEL analysis. To mention the most popular studies, Baber and Wen [8] introduced cyclic degradation, Baber and Noori [9] incorporated pinching, and Park et al. [10] covered biaxial bending. Several studies consider asymmetric hysteresis; proposals with increasing degree of flexibility, and complexity as well, are from Colangelo et al. [5], Wang and Wen [11], Song and Der Kiureghian [12]. Finally, Shih and Sung [13] implemented isotropic hardening.

Baber and Wen [14] and Baber [15] formulated a lumped-plasticity model for SEL analysis of hysteretic framed structures. This model consists in linearly elastic beam elements provided with zero-length rotational springs at the ends, whose moment-rotation relationship follows the Bouc-Wen law. Herein such a model is generalized in order to make the flexural strength of each spring dependent on the axial force in the beam, so that the interaction between resisting axial force and bending moment (PM interaction) can be taken into account. Piecewise linear approximation of the dependency between resisting biaxial bending moments has long been formulated following a general multivariate approach, in principle suitable for bending moment and axial force as well [16]. However, as far as the writer knows, any direct implementation into the Bouc-Wen model is still missing. Herein the PM interaction is incorporated into the Bouc-Wen model made asymmetric according to Colangelo et al. [5]. Analytic, closed-form relationship between the parameters of the equivalent linear system and those of its probabilistic response is preserved for efficiency. A preliminary validation of the proposed model is presented. Results from SEL analysis of two portal frames differing in the importance of PM interaction are compared with each other. The same results are also compared with those from MC simulation.

2. Extended Bouc-Wen model

As usual, two components, one linearly elastic and one hysteretic, are connected to each other in parallel. The behavioral model in terms of total bending moment M and flexural rotation θ of a zero-length spring writes

$$M = \alpha k_\theta \theta + (1-\alpha) k_z z \tag{1}$$

k_θ = stiffness of the linear component; k_z = alike parameter of the hysteretic component; α = parameter to weigh up the components, related to the post-yield hardening ratio; z = auxiliary variable to formulate the actual Bouc-Wen model. In this study, the formulation proposed to introduce PM interaction is

$$\dot{z} = \dot{\theta}\left\{a\, y^n(P) - |z|^n\left[\gamma + \beta\,\mathrm{sgn}(z\dot{\theta}) + \delta\,\mathrm{sgn}(z)\right]\right\} \tag{2}$$

a, n, γ, β = parameters to govern the hysteresis features as in the original Bouc-Wen model; δ = additional parameter for asymmetric strength according to Colangelo et al. [5]; $y(P)$ = novel function of axial force specific to the present study to introduce PM interaction. In detail, it is proposed to assume a second-degree parabola as follows

$$y(P) = 1 - \left(\frac{2P - P_{\max} - P_{\min}}{P_{\max} - P_{\min}} \right)^2 \qquad P_{\min} \le P \le P_{\max} \tag{3}$$

$P_{\min}$, $P_{\max}$ = extreme resisting axial force at pure tension and compression failure, respectively. Notice that y is dimensionless; the parameters in Eq. (2), including δ to introduce asymmetry if intended [5], govern the dimensional flexural strength. In fact, the positive and negative asymptotic values of the auxiliary variable, related to the resisting bending moments, are

$$z_y^{(\pm)} = \sqrt[n]{\frac{a}{\gamma + \beta \pm \delta}}\, y(P) \tag{4}$$

Setting $y(P) \equiv 1$ in Eq. (2) gives the previous model without PM interaction, symmetric ($\delta = 0$) or not ($\delta \neq 0$). Clearly, Eq. (3) requires the probability of axial force being external to the interval $[P_{\min}, P_{\max}]$ to be negligible. This is not guaranteed with Gaussian processes, as the usual SEL method assumes. Moreover, Eq.s (2) and (3) imply parabolic approximation of the PM interaction diagram. This is usual for steel members, but in the case of reinforced concrete the approximation may be good (Fig. 1a) or it may be poor, for asymmetric cross sections especially (Fig. 1b). As a possible remedy, if the PDF of axial force is negligible outside some interval smaller than $[P_{\min}, P_{\max}]$, then the parabola may be fitted over that interval. Finally, notice that the relationship $y(P)$ affects not only strength, but also stiffness accidentally. The greater is the exponent n (as it should be in order to tend to the elasto-plastic behavior), the greater is the stiffness decrease, which is not very rational.

3. Framed structure model

Planar framed structures are considered. Any beam element, arbitrarily oriented, has axial, flexural and shear linearly elastic behavior. Plastic deformation may occur in zero-length rotational springs placed in any end of each beam element, their constitutive law being Eq.s (1) to (3). Since the seismic response, e.g. the bending moment and yielding itself, is random, the hysteretic springs are placed in every critical region, even in those where the yielding probability is small [14][15]. Each spring implies that one rotation θ and one auxiliary variable z are introduced along with the nodal degrees of freedom (DOF's), which is relatively demanding. Obviously, the initial stiffness of the spring should be so great that rotation θ remains small unless actual yielding occurs. Moreover, one can calibrate reciprocally the stiffness of each beam element and the initial stiffness of its springs in order to reflect the flexural stiffness of the actual beam element in the elastic stage.

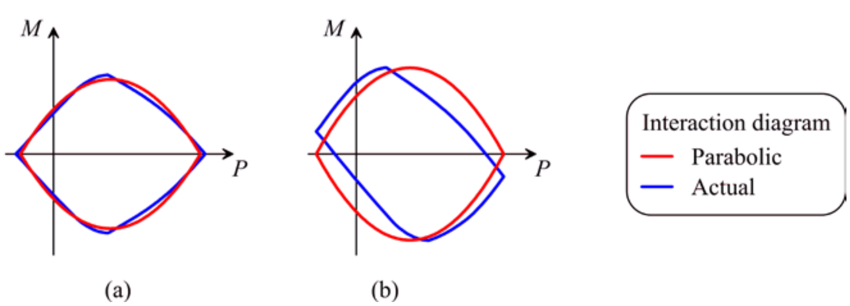

Fig. 1 – Approximation of interaction diagram: (a) symmetric cross section; (b) asymmetric cross section

The frame model described above is formulated as follows. First, the static and dynamic equilibrium equations of the frame joints write

$$\mathbf{M}\ddot{\mathbf{u}} + \mathbf{C}\dot{\mathbf{u}} + \mathbf{K}_{uu}\mathbf{u} - \mathbf{K}_{u\theta}\boldsymbol{\theta} = \mathbf{f}_{u,G} + \mathbf{f}_{u,E} \tag{5}$$

$\mathbf{u}$ = vector with translational and rotational DOF's of joints; $\boldsymbol{\theta}$ = vector with rotations of springs; $\mathbf{M}$ = mass matrix; $\mathbf{C}$ = viscous damping matrix; $\mathbf{K}_{uu}$ = stiffness matrix from assembling the beam matrices; $\mathbf{K}_{u\theta}$ = stiffness matrix to quantify the decrease in the linearly elastic reaction forces of the beam elements due to rotations $\boldsymbol{\theta}$ at their ends, obtained from assembling proper entries of the beam matrices; $\mathbf{f}_{u,G}$ = vector with nodal forces equivalent to the deterministic loads on the frame; $\mathbf{f}_{u,E}$ = vector with nodal forces representing the seismic action, idealized as a stationary zero-mean Gaussian white noise filtered twice.

Second, the bending moments at the beam ends must equal the moments in the springs

$$\mathbf{K}_{\theta u}\mathbf{u} - \mathbf{K}_{\theta\theta}\boldsymbol{\theta} - \mathbf{f}_{\theta,G} = \mathbf{A}\boldsymbol{\theta} + \mathbf{B}\mathbf{z} \tag{6}$$

$\mathbf{K}_{\theta u}$ = stiffness matrix that expresses the bending moments at the beam ends depending on the nodal DOF's, obtained from assembling proper entries of the beam matrices; $\mathbf{K}_{\theta\theta}$ = stiffness matrix to quantify the decrease in the linearly elastic bending moments at the beam ends due to rotations $\boldsymbol{\theta}$, obtained from assembling the flexural entries of the beam matrices; $\mathbf{f}_{\theta,G}$ = vector with nodal bending moments equivalent to the deterministic loads on the beams; $\mathbf{A}$, $\mathbf{B}$ = diagonal matrices with entries $\alpha_i k_{\theta i}$ and $(1-\alpha_i)k_{zi}$ from Eq. (1), respectively; $\mathbf{z}$ = vector with auxiliary variables. Notice that any inertial term does not appear in Eq. (6) because the mass is assumed to be lumped at the frame joints.

Finally, the hysteretic constitutive equations of the springs are expressed as follows

$$\dot{\mathbf{z}} = \mathbf{g}\left(z_i, \dot{\theta}_i, P_i(\mathbf{u})\right) \tag{7}$$

$\mathbf{g}$ = vector with nonlinear Eq.s (2) of every spring. It is a key point of the proposed model that each axial force P is assumed to depend linearly on the nodal translations in the vector $\mathbf{u}$. This relationship merely involves the axial stiffness of the beam element, which remains linearly elastic, and its direction cosines. Thus, the axial force level dictates the yielding moment level, but the model cannot capture crushing nor tension failure from axial force. Any interaction of axial and flexural inelastic strain is neglected. Within such an approximation, it holds

$$P_i(\mathbf{u}) = \mathbf{t}_i\mathbf{u} - f_{Pi} \tag{8}$$

$\mathbf{t}_i$ = row vector with the axial stiffness times the direction cosines of the beam element including the i-th spring, assembled in proper positions; f_{Pi} = deterministic equivalent nodal force in the axial direction of the same beam element, e.g. the column self-weight. Notice that Eq. (8) is elementary but its consequence is important in that some nonlinear Eq.s (7) couple through the translational DOF's associated with axial deformation. This applies to the springs of a same beam element and, possibly, of different beam elements adjoining a same node. On the other hand, any dependency on P vanishes and Eq.s (7) uncouple without PM interaction and $y(P) \equiv 1$ in Eq. (2).

4. Statistical equivalent linearization

The SEL technique in the non-zero mean case, herein due to deterministic load and asymmetric strength as well, follows Baber [17]. The present study is restricted to the stationary problem. Nevertheless, PM interaction as proposed herein seems not to preclude the usual technique for the non-stationary problem [18].

4.1 Mean values

The Gaussian processes **u**, **θ**, **z**, P_i are decomposed into zero-mean processes plus the respective mean value. Applying the expectation operator $E\{\cdot\}$ to Eq.s (5), (6) and (7) yields the equations for the mean values μ

$$\begin{cases} \mathbf{K}_{uu}\boldsymbol{\mu}_u - \mathbf{K}_{u\theta}\boldsymbol{\mu}_\theta = \mathbf{f}_{u,G} \\ \mathbf{K}_{\theta u}\boldsymbol{\mu}_u - (\mathbf{K}_{\theta\theta} + \mathbf{A})\boldsymbol{\mu}_\theta = \mathbf{f}_{\theta,G} + \mathbf{B}\boldsymbol{\mu}_z \\ E\left\{\mathbf{g}\left(z_{0i} + \mu_{zi}, \dot{\theta}_{0i}, P_{0i} + \mu_{Pi}\right)\right\} = \mathbf{0} \end{cases} \tag{9}$$

where subscript 0 denotes any zero-mean process. Similar transformation of Eq. (8) gives

$$\mu_{Pi} = \mathbf{t}_i \boldsymbol{\mu}_u - f_{Pi} \tag{10}$$

which subtracted from Eq. (8) yields

$$P_{0i} = \mathbf{t}_i \mathbf{u}_0 \tag{11}$$

However, it is not convenient to substitute the axial force P_{0i} in Eq. (9) with nodal translations, because PDF's involving a greater number of variables would appear. By elaborating the first two sets of Eq. (9) in order to eliminate $\boldsymbol{\mu}_\theta$, one obtains the relationship $\boldsymbol{\mu}_u = \boldsymbol{\mu}_u(\boldsymbol{\mu}_z)$, which substituted into Eq. (10) yields $\mu_{Pi} = \mu_{Pi}(\boldsymbol{\mu}_z)$; finally, such relationships are introduced into the third set of Eq. (9). At this point the third set of Eq. (9), the only one being nonlinear, can be solved apart to obtain the mean values of auxiliary variables $\boldsymbol{\mu}_z$. Each nonlinear equation of this kind can be written as follows (subscript i is omitted for the sake of brevity)

$$a e_a - \gamma e_\gamma - \beta e_\beta - \delta e_\delta = 0 \tag{12}$$

e_γ, e_β = expectations as in the original Bouc-Wen model [17]; e_δ = additional expectation appearing in the case of asymmetric strength [5]; e_a = novel expectation specific to the proposed extension for PM interaction. In detail, e_a vanishes without PM interaction, otherwise the parabolic assumption as in Eq. (3) leads to an expectation of polynomials with only two variables, which has the analytic, closed-form expression

$$e_a = \frac{\sigma_{\dot{\theta}}}{2\pi} \sum_{k=0}^{n} \binom{n}{k} (-1)^k \left(\frac{\sigma_P}{P_1}\right)^{2k} \sum_{l=0}^{2k} \binom{2k}{l} \left(\frac{\mu_P - P_2}{\sigma_P}\right)^{2k-l} \sum_{j=0}^{l} \binom{l}{j} \rho_{P\dot{\theta}}^{j} \left(1 - \rho_{P\dot{\theta}}^2\right)^{\frac{l-j}{2}} I(l-j)\, I(j+1) \tag{13}$$

σ = standard deviation; ρ = coefficient of correlation; $P_1 = (P_{\max} - P_{\min})/2$; $P_2 = (P_{\max} + P_{\min})/2$; finally, being $\Gamma(\cdot)$ the gamma function,

$$I(m) = \begin{cases} 2^{(m+1)/2}\,\Gamma\left[(m+1)/2\right] & m \text{ even integer or null} \\ 0 & m \text{ odd integer} \end{cases} \tag{14}$$

Once the mean values $\boldsymbol{\mu}_z$ are computed by solving Eq.s (12), the mean values $\boldsymbol{\mu}_u$, $\boldsymbol{\mu}_\theta$, μ_{Pi} derive immediately from the linear relationships in Eq.s (9) and (10). Obviously, preliminary estimation of the covariance matrix of the response processes is necessary.

4.2 Covariance matrix

Subtracting each set of Eq. (9) from the corresponding Eq. (5), (6) or (7) yields the equations for covariance

$$\begin{cases} \mathbf{M}\ddot{\mathbf{u}}_0 + \mathbf{C}\dot{\mathbf{u}}_0 + \mathbf{K}_{uu}\mathbf{u}_0 - \mathbf{K}_{u\theta}\boldsymbol{\theta}_0 = \mathbf{f}_{u,E} \\ \mathbf{K}_{\theta u}\mathbf{u}_0 - (\mathbf{K}_{\theta\theta} + \mathbf{A})\boldsymbol{\theta}_0 = \mathbf{B}\mathbf{z}_0 \\ \dot{\mathbf{z}}_0 - \mathbf{g}(z_{0i} + \mu_{zi}, \dot{\theta}_{0i}, P_{0i} + \mu_{Pi}) = \mathbf{0} \end{cases} \tag{15}$$

Except the mean values μ_{zi} and μ_{Pi} appearing in the nonlinear third set, Eq. (15) is the same as in a zero-mean problem. Each nonlinear equation can be linearized likewise (subscript *i* is omitted for the sake of brevity)

$$\dot{z}_0 = c_z z_0 + c_\theta \dot{\theta}_0 + c_P P_0 \tag{16}$$

The factors *c*'s are obtained by minimizing the mean squared error between this equivalent linear relationship and the nonlinear one, using the linear Gaussian solution [2]. Notice that since the axial force depends linearly on the nodal translations, Eq. (11), linearization with respect to P_0 as in Eq. (16) is the same as linearization with respect to $\mathbf{u}_0$. Similar to calculation of mean values, considering the axial force rather than the nodal translations is convenient because a lesser number of variables are involved. The factors *c*'s can be expressed as follows

$$\begin{aligned} c_z &= -\gamma c_{z\gamma} - \beta c_{z\beta} - \delta c_{z\delta} \\ c_\theta &= a c_{\theta a} - \gamma c_{\theta\gamma} - \beta c_{\theta\beta} - \delta c_{\theta\delta} \\ c_P &= a c_{Pa} \end{aligned} \tag{17}$$

$c_{z\gamma}$, $c_{z\beta}$, $c_{\theta\gamma}$, $c_{\theta\beta}$ = expectations as in the original Bouc-Wen model [17]; $c_{z\delta}$, $c_{\theta\delta}$ = additional expectations in the case of asymmetric strength [5]; $c_{\theta a}$, c_{Pa} = novel expectations. Without PM interaction, $c_{\theta a} \equiv 1$ and $c_{Pa} \equiv 0$; one obtains the former model. Otherwise, the parabolic assumption leads to the analytic, closed-form expressions

$$\begin{aligned} c_{\theta a} &= \frac{1}{\sqrt{2\pi}} \sum_{k=0}^{n} \binom{n}{k} (-1)^k \left(\frac{\sigma_P}{P_1}\right)^{2k} \sum_{l=0}^{2k} \binom{2k}{l} \left(\frac{\mu_P - P_2}{\sigma_P}\right)^{2k-l} I(l) \\ c_{Pa} &= \frac{n\sigma_{\dot{\theta}}}{\pi\sigma_P} \sum_{k=0}^{n-1} \binom{n-1}{k} (-1)^{k+1} \left(\frac{\sigma_P}{P_1}\right)^{2(k+1)} \sum_{l=0}^{2k+1} \binom{2k+1}{l} \left(\frac{\mu_P - P_2}{\sigma_P}\right)^{2k-l+1} \sum_{j=0}^{l} \binom{l}{j} \rho_{P\dot{\theta}}^{j} \left(1-\rho_{P\dot{\theta}}^2\right)^{\frac{l-j}{2}} \cdot \\ &\quad \cdot I(l-j)\, I(j+1) \end{aligned} \tag{18}$$

As usual, these factors depend also on the unknown response; an iterative approach to solution is necessary.

5. Numerical application and validation

The results from SEL analysis of two portal frames with and without the proposed PM interaction model are compared with i) one another and ii) MC simulation using the model implemented in the well-known computer code DRAIN [19]. Also the DRAIN model consists in linearly elastic beams with hysteretic springs at the ends, but it differs from the proposed model in other respects. In detail, each hinge is introduced into the frame after yielding occurs. Their behavior is elasto-plastic. The PM interaction curve is piecewise linear; overshooting is solved by subsequent equilibrium correction. Thus the present comparison is qualitative more than quantitative. Moreover, it is restricted to the zero-mean case with symmetric strength and without deterministic load.

Table 1 – Properties of portal frames (unit: m, kN, s)

Property	Frame A	Frame B
Height	3	3
Span	6	3
Column's cross section	0.3×0.3	0.3×0.3
Beam's cross section	0.3×0.5	0.3×0.39685
Young's modulus of elasticity	3×10^7	3×10^7
Total mass	12.848	12.848
Rayleigh's damping ratio	2%	2%

Table 2 – Parameters of the extended Bouc-Wen model (unit: m, kN, rad)

Member	α	$k_\theta \equiv a$	k_z	n	$\gamma \equiv \beta$	δ	P_{min}	P_{max}
Column	0.001	418162.50	1	1	2211.8526	0	−150	150
Beam	0.001	967968.75	1	1	6249.6557	0	—	—

5.1 Portal frames

Two portal frames hereafter called 'frame A' and 'frame B' are examined under horizontal seismic excitation (Table 1). In view of future analysis with the vertical component as well, 5% of the total mass is lumped at each beam-column joint, and 90% at midspan, where an additional node is put. Being the beam axially rigid, there are four dynamic translational DOF's. The frame B differs from the frame A in that the beam span and moment of inertia are halved. If all members were axially rigid, this would imply the same stiffness and bending moments due to a same horizontal action. Nevertheless, variation of axial force in the columns would double in the shorter frame B. Indeed, the columns are not axially rigid; however PM interaction is expected to be important for the frame B more than for the frame A, given that the mass and seismic action on the frames are the same.

The parameter values for the extended Bouc-Wen model are set as listed in Table 2. The corresponding PM interaction diagram for the column is shown in Fig. 2, compared with the piecewise linear diagram used for MC simulation with DRAIN. Notice that any variation of axial force decreases the column strength with respect to the initial one (recall that the gravity load is omitted herein). The maximum strength of the column is greater than the beam strength by a factor equal to 1.22; however the value of $|P_{min}| = P_{max}$ is so small that the column strength may become similar to the beam strength in the frame B with PM interaction at some seismic intensity. The load-displacement loop of the frame members modeled as a cantilever beam long one-half the member length is shown in Fig. 3. Notice that the values selected for the axial force in the column correspond to the maximum difference between the PM interaction diagrams (Fig. 2), yet the loops seem to be in reasonable agreement. Also notice that comparing the stiffness according to each model in Fig. 3, noticeable difference appears between the columns as $|P|$ increases, due to the influence of the function $y(P)$ on strength and stiffness as well, as mentioned in Section 2.

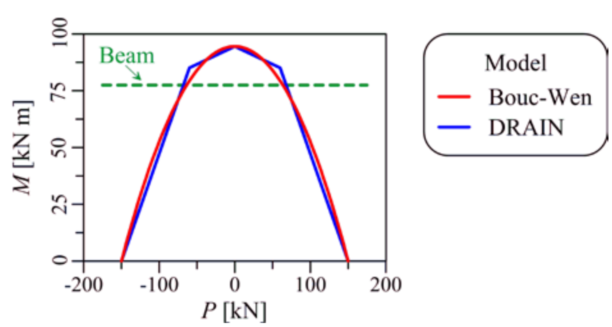

Fig. 2 – Interaction diagrams for SEL analysis and MC simulation

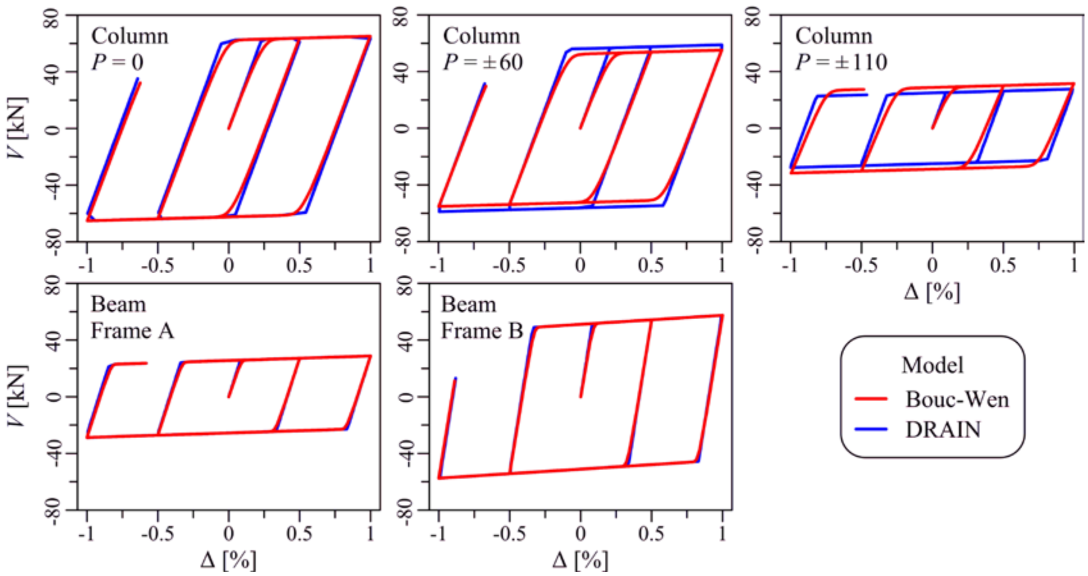

Fig. 3 – Force-displacement loops of frame members

5.2 Seismic action

A number of analyses are carried out with increasing intensity of the ground motion in the horizontal direction. The intensity measure is the power spectral density (PSD) level S_0 of the white noise to be filtered twice. However, results are illustrated in the following depending on the standard deviation of the filtered acceleration, which is more convenient than the white noise level.

The sample size for MC simulation is assumed to be equal to 100. The accelerograms are sampled Gaussian white noises made nonstationary by a deterministic modulating function and filtered in the frequency domain [20]. The total duration is assumed to be equal to 120 s; MC statistics are calculated over a 90 s long interval, taken within the stationary part of the accelerograms. Scaling might be such that the sample mean value of each discrete PSD of the nonstationary noises equals the intensity level S_0 of the stationary white noise in the corresponding SEL analysis. Indeed, in order to make MC simulation and SEL analysis as similar as possible, each accelerogram is scaled so that the sample standard deviation of its stationary part equals the standard deviation of the stationary process, from integration of its analytic PSD function.

The PSD functions of seismic input to SEL analysis and MC simulation as well are shown in Fig. 4, which also reports the values of the parameters of the two filters in series. In detail, the discrete PSD's of 100 artificial accelerograms generated as above have the sample mean illustrated in Fig. 4 provided that scaling is based on the intensity level S_0. Matching with the analytic PSD implicit in the SEL analysis is good. This would assure the frequency content be proper aside from intensity. In turn, intensity is deemed to be proper by scaling on the basis of the standard deviations mentioned above.

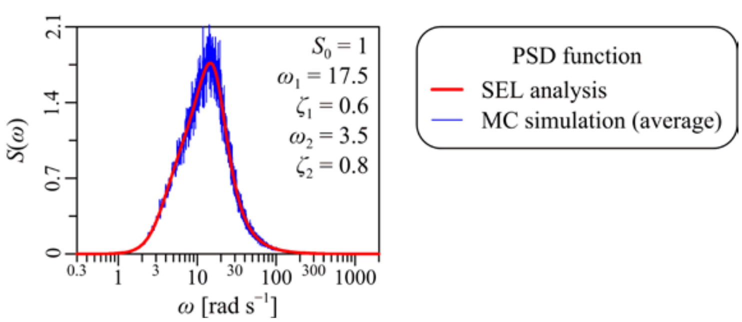

Fig. 4 – PSD's of ground acceleration

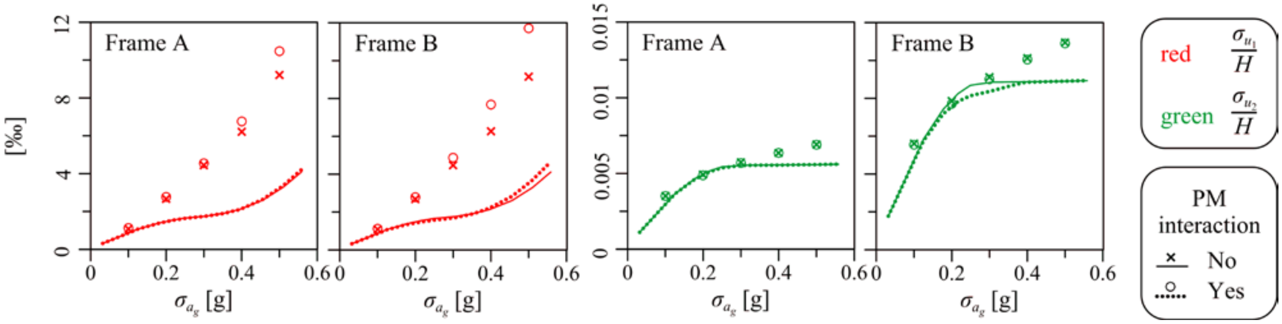

Fig. 5 – Nodal translations

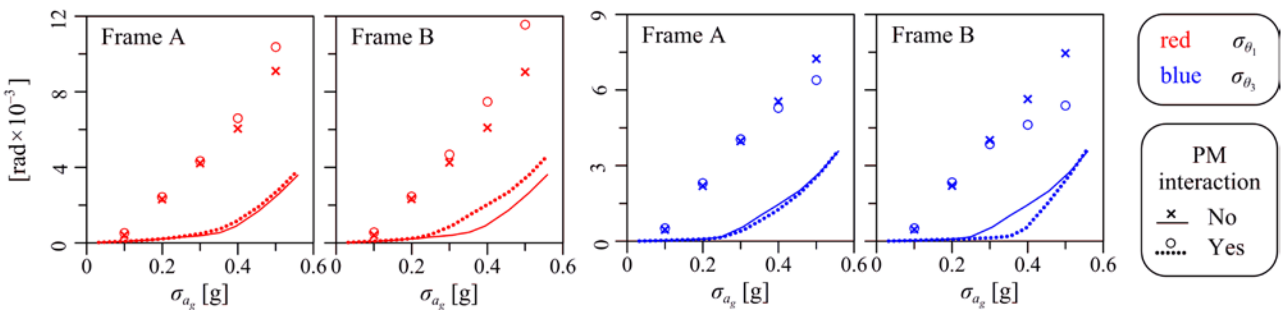

Fig. 6 – Hysteretic rotations

5.3 Results

The standard deviation of nodal displacements normalized by the frame height is shown in Fig. 5; u_1 denotes the horizontal translation, u_2 the vertical translation of the beam-column joint. The curves represent SEL analysis, the markers MC simulation. Notice that the frames have alike horizontal translation, but the vertical translation in the shorter frame B is greater than in the longer frame A, consistent with the axial force in the columns. The difference between SEL and MC results increases with increasing seismic intensity. This is reasonable because the greater the intensity, the greater the degree of yielding and nonlinearity, the greater the approximation of SEL analysis, aside from any difference between the models. Moreover, the SEL and MC vertical translations are not as different as the horizontal translations are, one would say because the frames yield in flexure while the column axial behavior remains linearly elastic. Importantly, the SEL and MC results agree on the effect of PM interaction. This effect is negligible on the vertical translation, but it causes the horizontal translation to increase. The greater the seismic intensity, the greater the variation in axial force, the greater is the increase and in the frame B more than in the frame A, as it must be. The only discordance appears that the effect of PM interaction on the horizontal translation of the frame A remains negligible according to SEL analysis, even with the greatest seismic intensity, whereas it becomes appreciable according to MC simulation.

The standard deviation of hysteretic rotations is shown in Fig. 6; θ_1 denotes rotation at the column bottom, θ_3 that at the beam end. Once again the difference between SEL and MC results is remarkable, except for the lowest seismic intensity; nevertheless there is reasonable agreement on the effect of PM interaction. With PM interaction, the column rotation increases because the column strength decreases; on the other hand, the beam rotation decreases. This effect is more pronounced on the frame B than on the frame A, as expected. Indeed, the effect on the frame A remains almost negligible according to SEL analysis, but not according to MC simulation. All in all, such results seem consistent with those about displacements in Fig. 5.

The mean value of hysteretic energies per unit of time from SEL analysis is shown in Fig. 7; subscript 1, 2 and 3 denote the column bottom, the column top and the beam end, respectively. Similar to the rotations above, with PM interaction the energy increases at the column bottom but it decreases at the beam end, in the frame B especially. The column top does not yield in fact. Notice that energy clearly shows that the onset of yielding is at $\sigma_{ag} \approx 0.2$ g. The SEL and MC results at 0.1 g are similar because the frames in essence are linearly elastic there.

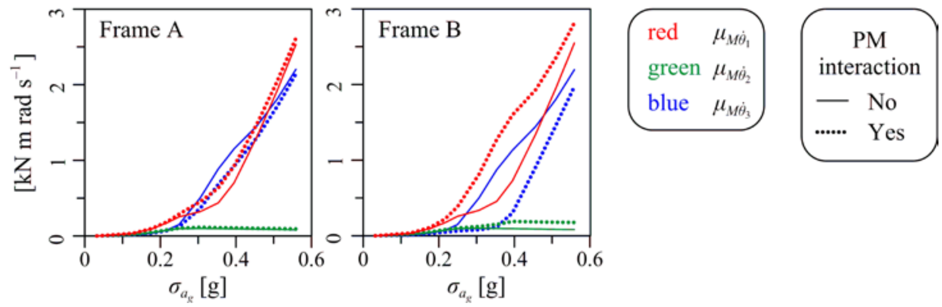

Fig. 7 – Hysteretic energies

The standard deviation of bending moments normalized by the respective yield moment is shown in Fig. 8; M_1 denotes moment at the column bottom, M_2 that at the column top (equal to the moment at the beam end, aside from the yield moment). The former moment is greater than the latter, so much so that the column bottom yields but the top does not. Beyond the yielding seismic intensity mentioned above, the results from SEL analysis stabilize, while excessive hardening appears from MC simulation. Nonetheless, in the frame B especially, the PM interaction causes decrease at the column bottom that yields, consistent with the interaction curve (Fig. 2). On the other hand, the PM interaction has no effect on the column top that in fact remains elastic.

The coefficient of correlation of the bending moment at the column bottom with the nodal translations u_1 and u_2 is shown in Fig. 9. Correlation from SEL analysis is almost perfect before yielding, as it must be because any moment and displacement is proportional to the seismic action. As the seismic intensity increases, this still holds for the vertical translation (notice the scale of vertical axes); instead, the correlation with the horizontal translation is lesser and lesser, in the frame B with PM interaction especially. Indeed, if the behavior were elasto-perfectly plastic then the correlation would vanish, because the strain would increase while the related stress would remain constant. One supposes that this might apply to the bending moment and horizontal translation, rather than the vertical one, because the frames yield in flexure whereas the columns remain linearly elastic with respect to axial behavior. In fact, MC simulation shows similar trends, except for a more pronounced decrease in correlation with the horizontal translation.

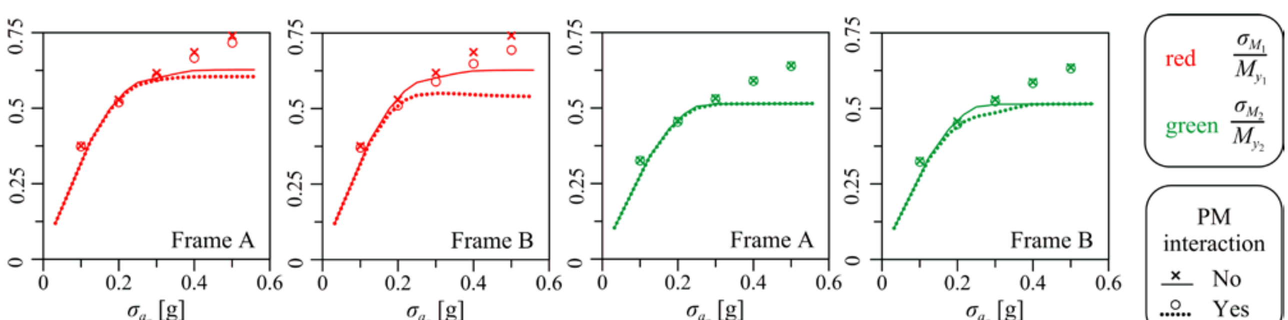

Fig. 8 – Bending moments

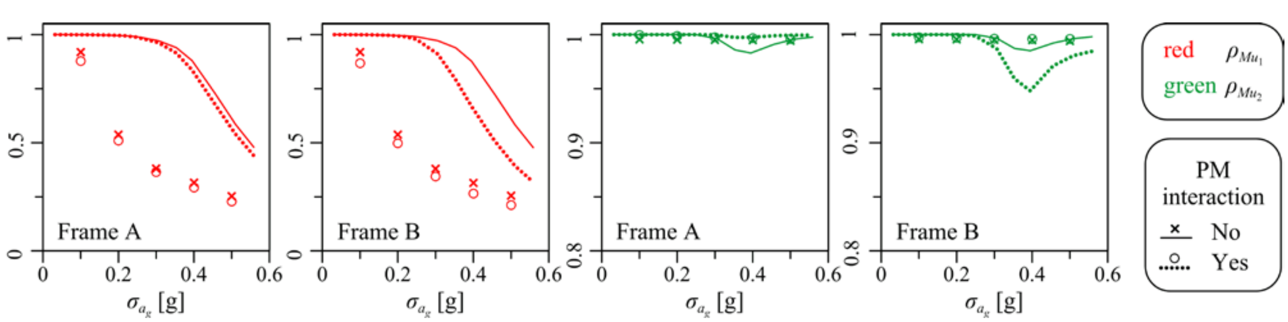

Fig. 9 – Coefficients of correlation between bending moment at column bottom and nodal translations

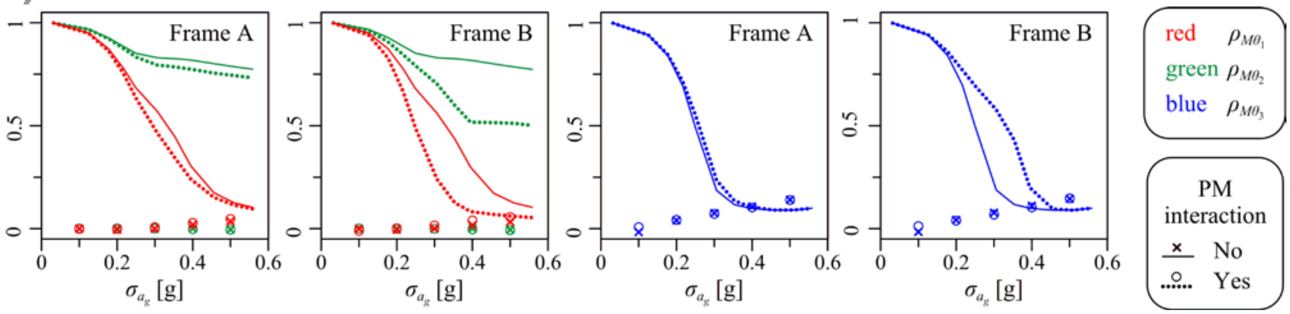

Fig. 10 – Coefficients of correlation between bending moment and corresponding hysteretic rotation

Finally, the coefficient of correlation between any bending moment and its corresponding hysteretic rotation is shown in Fig. 10; subscripts 1, 2 and 3 respectively denote the column bottom, the column top and the beam end. Contrary to all results presented previuosly, SEL analysis and MC simulation show a totally different picture. This is because the proposed model always incorporates all hysteretic springs into the frame (Section 3), whereas the DRAIN implementation introduces a hinge into a beam element end no sooner than deterministic yielding occurs there (Section 5).

According to SEL analysis, all correlations are almost perfect in the elastic stage. In fact, both bending moment and rotation increase with seismic intensity, although the rotation is supposed to do to a small extent because of great initial stiffness of the hysteretic spring. Then the correlation at the column bottom and that at the beam end steeply decrease around the yielding seismic intensity. Once more, the reason may be said to be the increase in the rotation against a bending moment that remains almost constant beyond yielding, hardening and PM interaction apart. In the frame B, the PM interaction causes the bending moment to decrease (Fig. 8) and rotation to increase (Fig. 6) at the column bottom; consistently, correlation in Fig. 10 decreases to the greatest extent there. In the frame B, the PM interaction causes rotation to decrease at the beam end, contrary to the column bottom (Fig. 6); consistently, correlation in Fig. 10 increases at the beam end. Significant correlation remains at the column top, which in fact should not yield; noticeable decrease even in such a correlation appears in the frame B with PM interaction.

According to MC simulation, any rotation is precisely zero before yielding, and correlation is null as well because the bending moment varies being constant (null) its corresponding rotation. Contrary to the SEL results, all correlations now vanish in the elastic stage. As the seismic intensity increases, the correlation at the column top, which does not yield, remains null. The correlation at the column bottom and, mostly, that at the beam end increase slightly. In fact, both the bending moment (Fig. 8) and rotation (Fig. 6) keep increasing. Finally, notice that at the greatest seismic intensity in Fig. 10 both SEL analysis and MC simulation show comparably small correlations at the column bottom and, mostly, at the beam end, that is where yielding occurs. All in all, even so different trends of these coefficients of correlation can be explained.

6. Conclusion

This study proposes an extension of the Bouc-Wen hysteresis model in order to introduce the PM interaction in the columns of planar framed structures subjected to earthquakes. A key feature is modelling the PM interaction diagram as parabolic. This leads to developing an analytic, closed-form formulation for an effective approach to probabilistic seismic analysis by means of the SEL method.

At present, a preliminary numerical validation of the model has been carried out. The results from SEL analysis of two portal frames are compared with one another and with the results from MC simulation as well. This is not an exhaustive validation, mainly because it is restricted to the zero-mean case. However, in such a case a number of response quantities compare successfully: the nodal displacements, hysteretic rotations, dissipated energies, and several coefficients of correlation. Where the effect of PM interaction is expected to be more pronounced due to the aspect ratio of the frame, this effect appears to be stressed in fact. All results are reasonable and consistent with those from MC simulation using a different PM interaction model.

Such results are encouraging and motivate one to carry out further validation. Provided that confirmation of the present findings will hold, there would be available a more realistic model for the probabilistic analysis of framed structures with column yielding. Application might be to a number of matters e.g.: i) effectiveness of the flexural capacity design provisions by the design codes; ii) importance of the vertical component of the ground motion; iii) estimation of the local ductility demand to the critical region connecting column and foundation.

7. Acknowledgement

Funding was in part by the Italian Department of Civil Protection within the DPC-ReLUIS 2016 project, task 6.

8. References

[1] Li J, Chen J (2009): *Stochastic Dynamics of Structures*. Wiley.

[2] Crandall SH (2006): A half-century of stochastic equivalent linearization. *Structural Control & Health Monitoring*, **13** (1), 27-40.

[3] Socha L (2008): *Linearization Methods for Stochastic Dynamic Systems*. Springer.

[4] Der Kiureghian A, Fujimura K (2009): Nonlinear stochastic dynamic analysis for performance-based earthquake engineering. *Earthquake Engineering & Structural Dynamics*, **38** (5), 719-738.

[5] Colangelo F, Giannini R, Pinto PE (1996): Seismic reliability analysis of reinforced concrete structures with stochastic properties. *Structural Safety*, **18** (2/3), 151-168.

[6] Bouc R (1967): Forced vibration of mechanical systems with hysteresis. *4th International Conference on Non-linear Oscillations*, Prague, Czechoslovakia.

[7] Wen Y-K (1976): Method for random vibration of hysteretic systems. *Journal of Engineering Mechanics Division*, **102** (EM2), 249-263.

[8] Baber TT, Wen Y-K (1981): Random vibration of hysteretic degrading systems. *Journal of Engineering Mechanics*, **107** (6), 1069-1087.

[9] Baber TT, Noori MN (1985): Random vibration of degrading, pinching systems. *Journal of Engineering Mechanics*, **111** (8), 1010-1026.

[10] Park YJ, Wen Y-K, Ang AH-S (1986): Random vibration of hysteretic systems under bi-directional ground motions. *Earthquake Engineering & Structural Dynamics*, **14** (4), 543-557.

[11] Wang CH, Wen Y-K (2000): Evaluation of pre-Northridge low-rise steel buildings—I: modeling. *Journal of Structural Engineering*, **126** (10), 1160-1168.

[12] Song J, Der Kiureghian A (2006): Generalized Bouc-Wen model for highly asymmetric hysteresis. *Journal of Engineering Mechanics*, **132** (6), 610-618.

[13] Shih M-H, Sung W-P (2005): A model for hysteretic behavior of rhombic low yield strength steel added damping and stiffness. *Computers & Structures*, **83** (12-13), 895-908.

[14] Baber TT, Wen Y-K (1982): Stochastic response of multistorey yielding frames. *Earthquake Engineering & Structural Dynamics*, **10** (3), 403-416.

[15] Baber TT (1986): Nonzero mean random vibration of hysteretic frames. *Computers & Structures*, **23** (2), 265-277.

[16] Casciati F, Faravelli L (1988): Stochastic equivalent linearization for 3-D frames. *Journal of Engineering Mechanics*, **114** (10), 1760-1771.

[17] Baber TT (1984): Nonzero mean random vibration of hysteretic systems. *Journal of Engineering Mechanics*, **110** (7), 1036-1049.

[18] Roberts JB, Spanos PD (1990): *Random Vibration and Statistical Linearization*. Wiley.

[19] Powell GH (1973): DRAIN-2D user's guide. *Report UCB/EERC-73/22*, University of California, Berkeley, USA.

[20] Clough RW, Penzien J (2003): *Dynamics of Structures*. Computers & Structures Inc, 2nd edition.